



ELSEVIER

SCIENCE @ DIRECT®

wasteWmanagement

Waste Management xxx (2005) xxx–xxx

www.elsevier.com/locate/wasman

2 Methane flux and oxidation at two types of intermediate landfill covers

3 Tarek Abichou ^{a,*}, Jeffery Chanton ^b, David Powelson ^b, Jill Fleiger ^b, Sharon Escoriaza ^a,
4 Yuan Lei ^a, Jennifer Stern ^c

5 ^a Department of Civil and Environmental Engineering, Florida A&M University, Florida State University, College of Engineering, Tallahassee,
6 FL 32310, USA

7 ^b Department of Oceanography, Florida State University, Tallahassee, FL 32306, USA

8 ^c Department of Geology, Florida State University, Tallahassee, FL 32306, USA

9 Accepted 17 November 2005
10

11 Abstract

12 Methane emissions were measured on two areas at a Florida (USA) landfill using the static chamber technique. Because existing lit-
13 erature contains few measurements of methane emissions and oxidation in intermediate cover areas, this study focused on field measure-
14 ment of emissions at 15-cm-thick non-vegetated intermediate cover overlying 1-year-old waste and a 45-cm-thick vegetated intermediate
15 cover overlying 7-year-old waste. The 45 cm thick cover can also simulate non-engineered covers associated with older closed landfills.
16 Oxidation of the emitted methane was evaluated using stable isotope techniques. The arithmetic means of the measured fluxes were 54–
17 2 g CH₄ m⁻² d⁻¹ from the thin cover and the thick cover, respectively. The peak flux was 596 g m⁻² d⁻¹ for the thin cover and
18 330 g m⁻² d⁻¹ for the thick cover. The mean percent oxidation was significantly greater (25%) at the thick cover relative to the thin cover
19 (14%). This difference only partly accounted for the difference in emissions from the two sites.

20 Inverse distance weighing was used to describe the spatial variation of flux emissions from each cover type. The geospatial mean flux
21 was 21.6 g m⁻² d⁻¹ for the thick intermediate cover and 50.0 for the thin intermediate cover. High emission zones in the thick cover were
22 fewer and more isolated, while high emission zones in the thin cover were continuous and covered a larger area. These differences in the
23 emission patterns suggest that different CH₄ mitigation techniques should be applied to the two areas. For the thick intermediate cover,
24 we suggest that effective mitigation of methane emissions could be achieved by placement of individualized compost cells over high emis-
25 sion zones. Emissions from the thin intermediate cover, on the other hand, can be mitigated by placing a compost layer over the entire
26 area.

27 © 2005 Published by Elsevier Ltd.
28

29 1. Introduction and background

30 In the USA, landfill emissions are 30% of the anthropo-
31 genic input to atmospheric methane (Hogan, 1993). The
32 imbalance between sources and sinks of CH₄ in the global
33 budget is less than 6% of the total of global sources (Dlu-
34 gokencky et al., 1994) or perhaps even approaching bal-
35 ance (Dlugokencky et al., 1998; Etheridge et al., 1998).
36 Therefore, a small decrease in CH₄ source strength could
37 result in stabilization of atmospheric CH₄, or, even better,

in a reduction in the atmospheric concentration (Lelieveld 38
et al., 1998; Thompson et al., 1992). As CH₄ is a more 39
potent greenhouse agent than is CO₂, lowering the atmo- 40
spheric CH₄ concentration is a very realistic and worth- 41
while goal. The relatively short residence time of CH₄ in 42
the atmosphere (7–10 yr) relative to CO₂ (100 yr) means 43
that the effects of mitigation efforts would be rapidly 44
observed. 45

Landfills can emit methane at rates varying from 0.0004 46
to 4000 g m⁻² d⁻¹ (Bogner and Spokas, 1993; Bogner et al., 47
1997; Czepiel et al., 1996; Borjesson and Svensson, 1997; 48
Chanton and Liptay, 2000). Bogner and Matthews (2003) 49
used a model that linked per capita waste generation with 50
per capita energy consumption and estimated global 51

* Corresponding author. Tel.: +1 850 410 6661; fax: +1 850 410 6142.
E-mail address: abichou@eng.fsu.edu (T. Abichou).

emissions of methane to be 16.4–18.1 Tg/y. This flux represents a conglomeration of point sources and as such could be readily mitigated. The global landfill emission estimated by Bogner and Matthews is about 3.5% of the total global methane emission of 500 Tg/y (Fung et al., 1997). Previous estimates of global landfill emissions were 40 Tg/y, 8% of the total (Fung et al., 1997). The IPCC IPCC, 2001 estimates that landfill emissions are 7% of global methane emissions.

Active landfills generally include areas with final cover, areas with intermediate cover, and areas with daily cover. Emissions of methane to the atmosphere can occur from all of these areas and at different rates. Towards this goal, the object of the study was to evaluate methane emissions and oxidation at two different types of landfill covers, a 45 cm thick intermediate cover consisting of a soil layer (sandy clay) overlain with well-vegetated topsoil, and a 15 cm thick non-vegetated intermediate soil cover. The 15 cm thickness is also a typical thickness for daily cover for state-approved programs under RCRA subtitle D provisions. Previous literature indicates that thicker soil covers reduce methane emissions, at least partly due to increased methane oxidation. We hypothesized that the flux from the thicker cover would be more patchy and dominated by hotspots, while the flux from the thinner cover would be higher but more uniform.

2. Methods

2.1. Site description

Measurements were performed at an MSW landfill which had no gas extraction system, located in Leon County, FL, USA (Chanton and Liptay, 2000). Two different locations for detailed sampling were selected for measurements associated with this paper. The first location, designated S1-Grid, had 7-year-old waste covered with about 45 cm of sandy clay and sandy loam. The area was thickly vegetated and entirely covered with a mixture of local grasses and occasional shrubs. A second location, designated S4-Grid, had 1-year-old waste covered with about 15 cm of sandy clay and is representative of a daily cover.

The S1-Grid was 60.8 m (200 ft) on a side and was divided into 64 squares, 7.6 by 7.6 m (25 by 25 ft). The S4-Grid was 64 m (210 ft) on a side and was also divided into 64 squares, 8 by 8 m (26 by 26 ft). Methane emissions were measured in the middle of each grid square. Additional locations (inside selected squares) were sampled at shorter distances to better define the flux spatial variability at small distances. The average flux was used for locations where the flux was repeatedly measured. For the S1-Grid, six squares had additional sampling locations in each quadrant, as well as one in the middle. In these squares, the minimum separation distance between sampling locations was 2.69 m (8.84 ft). For the S4-Grid, two squares had 12 additional sampling locations with a 1–8 m separation. Flux

measurements and stable isotope testing to determine methane oxidation at the S1-Grid were conducted from September 2003 to February 2004. Measurements at the S4-Grid were conducted from February 2004 to May 2004.

2.2. Methane emission rates and gas analysis

Methane emission rates from the landfill surface were determined using a static chamber technique. Static chambers are the most frequently used technique for the measurement of gas fluxes from soils. The chamber technique is low in cost, simple to operate and especially useful for addressing research objectives needing spatial and temporal variability of fluxes at a small scale. Chambers are particularly well suited to in situ studies addressing physical, chemical and biological controls on surface-atmosphere trace gas exchange (Livingston and Hutchinson, 1995). The principle of static chambers is to seal a volume above a gas-emitting or consuming surface such that the emitted (or consumed) gas cannot escape and its accumulation in the volume can be monitored. The chambers used in this study were constructed with polished aluminum sheeting and have dimensions of $0.63 \times 0.63 \times 0.2$ m (covering an area of 0.4 m^2). They contained a small fan to circulate air inside the chamber. Chambers were sealed to the ground by firming soil around the outside or by clamping them to pre-installed collars. Methane samples were collected from a chamber immediately after sealing (time 0) and after 2, 5, 10, and 15 min using 60-mL plastic syringes fitted with plastic valves. Chamber air was sampled via a 1 m long 1/8 in. plastic tube sealed at the outward end with a valve. Samples were analyzed on a gas chromatograph equipped with a flame ionization detector within 4 h of collection. Methane flux was determined from concentration data (C in ppmv) plotted versus elapsed time (t in minutes). The data generally fit a linear relationship, in which case dC/dt is the slope of the fitted line. The methane flux, F ($\text{g}/\text{m}^2/\text{d}$), was then calculated as follows:

$$F = PVMU(dC/dt)/(ATR), \quad (1)$$

where P is pressure (atm), V is chamber volume (80 L, plus collar volume), M is the molar mass of methane (16 g/mol), U is the units conversion factor ($0.00144 \text{ L min}/(\mu\text{L d})$), A is the area covered by the chamber (0.4 m^2), T is chamber temperature (K), and R is the gas constant ($0.08205 \text{ L atm}/(\text{Kmol})$). The slope of the line, dC/dt , was determined by linear regression between CH_4 concentration and elapsed time. Following the approach of Barlaz et al. (2004), a non-zero flux was reported only if there was 90% confidence ($p < 0.1$) in the correlation between CH_4 concentration and time, otherwise a zero-flux is reported.

2.3. Geospatial analysis

Two commonly used interpolation methods are kriging and inverse distance weighing (IDW). In kriging, a model of the overall spatial measured variance structure is used

159 to generate the interpolated contours. The measured
 160 variance structure is shown as a variogram with half the
 161 variance on the y -axis and sample separation distance on
 162 the x -axis. Key variables for a variogram are the nugget
 163 (unexplained or error variance), sill (total model variance,
 164 equal to nugget plus “scale”), and range (distance where
 165 the variance reaches the sill) (Yates and Warrick, 2002).
 166 In IDW, the interpolation contours are calculated by
 167 weighing neighbouring data using the inverse of the separa-
 168 tion distance to a power. IDW uses weighted averaging
 169 techniques to fill the elevation matrix. The interpolated
 170 value of a cell is determined from values of nearby data
 171 points taking into account the distance of the cell from
 172 those input points. Weights are inversely proportional to
 173 the power (p) of the distance. A power value of “2” is com-
 174 monly used for mapping mountainous terrains with sharp
 175 peaks (Surfer, 2002) and was selected for our analysis.
 176 IDW is considered an exact interpolator because the model
 177 value equals the measured value at a measurement point.
 178 Spokas et al. (2003) compared IDW with kriging in inter-
 179 polating methane flux data and reported that IDW is an
 180 acceptable method to map methane flux emissions from
 181 landfill surfaces. Abichou et al. (2005) reported that IDW
 182 resulted in similar geospatial emissions to those obtained
 183 using kriging.

184 A three-dimensional surface was created using the flux
 185 contour map obtained with IDW over the sampled area.
 186 Fig. 1 shows a typical surface created using IDW. The total
 187 volume of positive emissions from the entire area was then
 188 obtained by calculating the volume of the positive side of
 189 flux contour map (Fig. 1). The total volume of negative
 190 emissions or (uptake by the cover) was obtained by calcu-
 191 lating the volume of the negative portion of the same con-
 192 tour map (Fig. 1). The net volume of emissions from the
 193 entire area is then calculated by subtracting the volume
 194 of the negative portion of the flux contour from the posi-
 195 tive portion of the same map. The geospatial mean was cal-
 196 culated by dividing the net emissions by the area. The flux
 197 contours were also divided into emission zones (high, med-
 198 ium, and low emission zones). All modeling and quantity

199 calculations were performed using Surfer (2002), developed
 200 by Golden Software, Inc., Golden, CO.

2.4. Stable isotopes: methane oxidation

202 Recently, stable carbon isotopic analysis of methane has
 203 been employed to quantify the oxidation of methane in
 204 landfill cover soils (Bergamaschi et al., 1998; Liptay
 205 et al., 1998; Chanton and Liptay, 2000; Borjesson et al.,
 206 2001; and Christophersen et al., 2001.) There are two stable
 207 isotopes of carbon, ^{12}C , which comprises 99% of carbon
 208 atoms and ^{13}C , which is about 1% abundant. Carbon iso-
 209 topic composition is expressed in the δ notation ($\delta^{13}\text{C}$),
 210 which is defined as follows:

$$212 \delta\text{‰} = ((R_{\text{sample}}/R_{\text{standard}}) - 1) \times 1000, \quad (2)$$

213 where R_{sample} is the $^{13}\text{C}/^{12}\text{C}$ ratio of the sample and
 214 R_{standard} is the $^{13}\text{C}/^{12}\text{C}$ ratio of the marine carbonate stan-
 215 dard (Pee Dee Belemnite (PDB), $R_{\text{standard}} = 0.01124$). Typ-
 216 ical landfill microbial CH_4 is produced at values below
 217 -55‰ (Chanton et al., 1999). Following partial oxidation,
 218 residual CH_4 may exhibit ^{13}C enriched values of -30 to
 219 -50‰ . Typical organic matter is ^{13}C enriched relative to
 220 CH_4 with a $\delta^{13}\text{C}$ value of -25‰ . The negative δ value indi-
 221 cates that the sample is ^{13}C depleted relative to the carbon-
 222 ate standard. The more negative the value, the more ^{13}C
 223 depletion is indicated.

224 In order to calculate the isotope ratio of the methane
 225 emitted (δ_E) from the soil during flux sampling, it was nec-
 226 essary to account for the local atmospheric methane pres-
 227 ent in the air within the chamber at the initiation of the
 228 emission measurement:

$$229 \delta_E = \frac{(\delta_F c_F) - (\delta_I c_I)}{c_F - c_I}, \quad (3)$$

232 where δ_I and c_I are the methane δ and concentration for the
 233 initial gas sample taken from the chamber, and δ_F and c_F
 234 refer to the final sample.

235 Significant isotopic fractionation occurs when methane
 236 is oxidized. Microbial culture studies have shown that

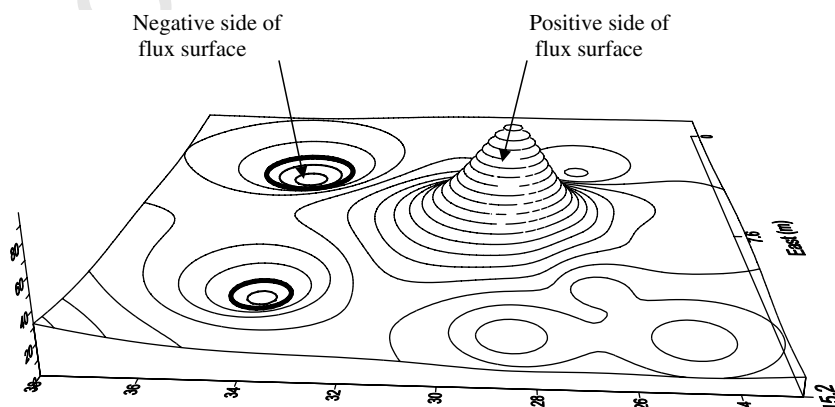


Fig. 1. Typical contour surface map obtained by Surfer. Note: Net emissions from the shown surface is volume of positive emissions minus the volume of negative emissions.

237 methanotrophic organisms preferentially consume CH₄
 238 containing the lighter isotope ¹²C, leaving residual CH₄
 239 enriched in ¹³C (Coleman et al., 1981; Barker and Fritz,
 240 1981). With an estimate of the preference of the bacteria
 241 for the lighter isotope, α_{ox}, one may calculate the extent
 242 of oxidation from the isotopic difference between the unaf-
 243 fected (anoxic zone methane) and the residual (or left over)
 244 methane which has been exposed to oxidation but not itself
 245 oxidized. The percentage of CH₄ oxidized in transit
 246 through the cover soil (f_o%) is determined by the following
 247 equation which describes isotopic fractionation in an open
 248 system:

$$251 f_o\% = 0.1(\delta_E - \delta_A)/(\alpha_{ox} - \alpha_{trans}), \quad (4)$$

252 where δ_A is the δ¹³C value of anoxic zone CH₄ (−55.4‰
 253 determined from soil probe data), α_{ox} is the isotopic frac-
 254 tionation factor for bacterial oxidation and α_{trans} is the iso-
 255 topic fractionation associated with gas transport. To the
 256 extent that gas transport is dominated by advection of
 257 gases across the landfill cap, α_{trans} will approach 1. How-
 258 ever, if diffusion plays a significant role in gas transport,
 259 α_{trans} will be greater than 1 causing this approach to yield
 260 conservative values of methane oxidation (De Visscher
 261 et al., 2004). We assumed that gas transport across the
 262 landfill surface was dominated by advection so that α_{trans}
 263 approached 1. This is a reasonable assumption because
 264 there was no gas collection system at this landfill so gas
 265 pressure should be greater within the landfill due to CH₄
 266 and CO₂ production. Consistent with this assumption,
 267 Czepiel et al. (2003) reported a strong negative relationship
 268 between landfill methane emission and atmospheric pres-
 269 sure. Bergamaschi et al. (1998) also observed that landfill
 270 gas transport is dominated by advection.

271 The fractionation factor (α_{ox}) was determined from soil
 272 temperature (T, °C) using the regression equation for α_{ox}
 273 with temperature for clay soil at this same landfill, reported
 274 in Chanton and Liptay (2000):

$$276 \alpha_{ox} = -0.000433T + 1.0421. \quad (5)$$

277 Stable isotopic ratios were determined using a Hewlett
 278 Packard Gas Chromatograph coupled via a combustion
 279 interface to a Finnegan Mat Delta S Isotope Ratio Mass
 280 Spectrometer (GCC–IRMS) following methods adapted
 281 from Merritt et al. (1995). For low-concentration samples
 282 (less than 1000 ppmv), a cryogenic focusing device was
 283 used on the front end of the gas chromatograph. The stan-
 284 dard deviation for replicate analyses of standards and sam-
 285 ples is generally 0.15‰ (Chanton et al., 1999). Stable
 286 isotopic ratios for the anoxic gases were determined using
 287 direct injection on the GCC–IRMS.

288 3. Results and discussion

289 3.1. Measured methane flux emissions

290 Eighty-eight flux measurements were performed in the
 291 S1-Grid and 76 flux measurements were performed in the

S4-Grid (Table 1). The minimum measured methane flux
 292 was −6.07 g m^{−2} d^{−1} for the S1-Grid and −4.22 g m^{−2} d^{−1}
 293 in the S4-Grid. Negative values indicate areas where meth-
 294 ane in the atmosphere was taken up by the soil and vegeta-
 295 tion. The peak measured flux was 330 g m^{−2} d^{−1} in the S1-
 296 Grid area and 596 g m^{−2} d^{−1} in the S4-Grid area. The
 297 mean flux was 21.6 g m^{−2} d^{−1} and 53.6 g m^{−2} d^{−1} for the
 298 S1-Grid and S4-Grid, respectively. The median flux was
 299 1.6 g m^{−2} d^{−1} for the S1-Grid and 3.3 g m^{−2} d^{−1} for the
 300 S4-Grid. A small number of high flux values resulted in
 301 skewed flux distributions.
 302

303 Measured fluxes were grouped into three categories
 304 (low, medium, and high). The S1-Grid had 67 (76%) mea-
 305 sured low fluxes, below 10 g m^{−2} d^{−1} (including negative
 306 fluxes), while the S4-Grid area had only 43 (51%). The
 307 number of measured medium methane fluxes (falling
 308 between 10 and 25 g m^{−2} d^{−1}) was 6 (7%) for the S1-Grid
 309 and 13 (17%) for the S4-Grid. The S1-Grid area had 15
 310 (17%) fluxes higher than 25 g m^{−2} d^{−1} and the S4-Grid area
 311 had 21 (26%) fluxes higher than 25 g m^{−2} d^{−1}. Table 1
 312 shows that 76% of the fluxes measured from the area rep-
 313 resentative of thick intermediate cover can be classified as
 314 low fluxes. On the other hand, only 57% of the fluxes mea-
 315 sured on the thin intermediate cover area can be classified
 316 as low fluxes.

317 3.2. Methane oxidation at landfill surface

318 Anoxic zone methane δ¹³C varied from −55.0 to 318
 319 −55.7‰ across the landfill (Table 2) and was similar to
 320 values reported by Chanton and Liptay (2000). Chanton
 321 and Liptay (2000) reported no seasonal variation in
 322 anoxic gas methane δ¹³C as it is produced within the
 323 landfill where seasonal temperature variation is muted
 324 by the heat generated by the decay of organic matter.
 325 There was no difference in anoxic zone methane at the
 326 two sites. The δ¹³C of the emitted methane, calculated
 327 from chamber initial and final isotope values using Eq.
 328 (3), varied from −34.5 to −54.8‰. The fraction of meth-
 329 ane oxidized during transit across the soil was calculated
 330 using Eq. (4). The mean fraction of oxidation was 25.2%

Table 1
 Summary of descriptive statistics of flux data

	S1-Grid		S4-Grid	
Number of tests	88		76	
Methane flux (g m ^{−2} d ^{−1})				
Minimum	−6.07		−4.22	
Median	1.63		3.33	
Maximum	329.98		595.86	
Mean	21.64		53.60	
Standard error	5.91		12.91	
Flux range	Number	%	Number	%
Low ^a (<10 g m ^{−2} d ^{−1})	67	76	43	57
Medium (10–25 g m ^{−2} d ^{−1})	6	7	12	16
High (>25 g m ^{−2} d ^{−1})	15	17	21	27

^a Low fluxes include negative fluxes.

Table 2
Methane isotope (δ) and oxidation results

n	S1-Grid					S4-Grid			
	Probes ^a								
	2	31				15			
	δ_A	δ_I	δ_F	δ_E	Oxidation (%)	δ_I	δ_F	δ_E	Oxidation (%)
Maximum	-55.02	-46.02	-42.02	-34.53	63.9	-47.59	-43.78	-42.21	43.2
Median	-55.38	-53.75	-51.97	-48.95	20.9	-50.13	-52.24	-52.11	10.7
Minimum	-55.73	-67.18	-59.41	-54.81	2.0	-71.00	-57.43	-57.91	-8.3
Mean	-55.38	-55.51	51.87	-47.64	25.2	-53.26	-51.40	-50.98	14.4
Standard deviation	0.50	5.61	4.70	5.08	15.7	7.89	3.83	4.65	15.2

δ_I is the CH_4 $\delta^{13}\text{C}$ for the initial gas sample taken from the chamber, and δ_F refers to the final sample. δ_A is anoxic CH_4 $\delta^{13}\text{C}$ and δ_E is calculated with Eq. (3).

^a Gas taken from 61 to 91 cm below surface.

331 for the S1-Grid and 14.4% for the S4-Grid (Table 2). The
332 peak oxidation rate was 63.9% for the S1-Grid and 43.2%
333 for the S4-Grid. Analyses of variance (ANOVAs) were
334 performed to determine significant differences in oxidation
335 among the two grid locations. Sample sizes were different;
336 consequently unbalanced, one-way ANOVAs were per-
337 formed. In this analysis, each sampling location was con-
338 sidered to be an independent sample. The F -value was
339 4.85 ($df = 1,44$, $p = 0.033$). A Duncan multiple range test
340 ($p = 0.05$) showed that oxidation in the S1-Grid
341 (mean = 25.2%) was significantly greater than in the S4-
342 Grid (mean = 14.4%). It should be noted that although
343 methane oxidation was significantly greater at the S1-Grid
344 site, this difference is not sufficient to explain the greater
345 CH_4 emission rates at the S4-Grid.

3.3. Geospatial methane flux emissions

346
347 The contours of CH_4 emissions from both areas show
348 the existence of circular patterns associated with high fluxes
349 using IDW (Figs. 2 and 3). A circular pattern demonstrates
350 that extremely high peak values are obtained using IDW,
351 whereas in kriging they tend to be smoothed downward.
352 IDW contours also show that a single extreme point or
353 clusters of dissimilar points have an effect on the contours.
354 In spite of not being as smooth as contours obtained by
355 kriging, Abichou et al. (2005) and Spokas et al. (2003)
356 reported that IDW is an acceptable and significantly simpler
357 method to map methane flux emissions from landfill
358 surfaces. They also reported that IDW resulted in similar
359 geospatial mean values when compared to kriging.

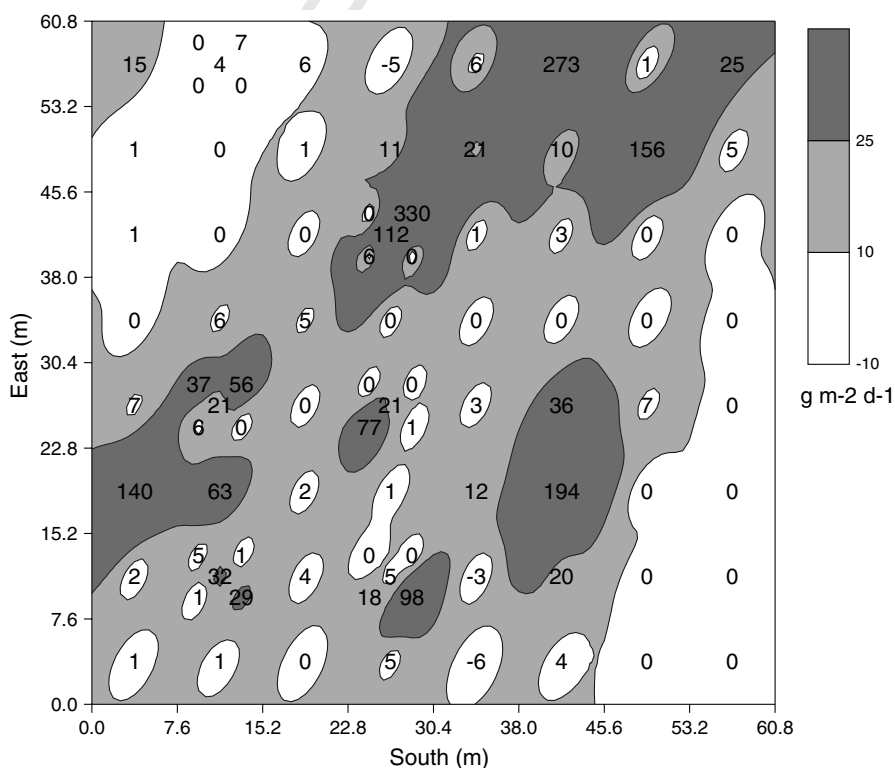


Fig. 2. S1-Grid Flux ($\text{g m}^{-2} \text{d}^{-1}$) contours obtained using inverse distance weighting.

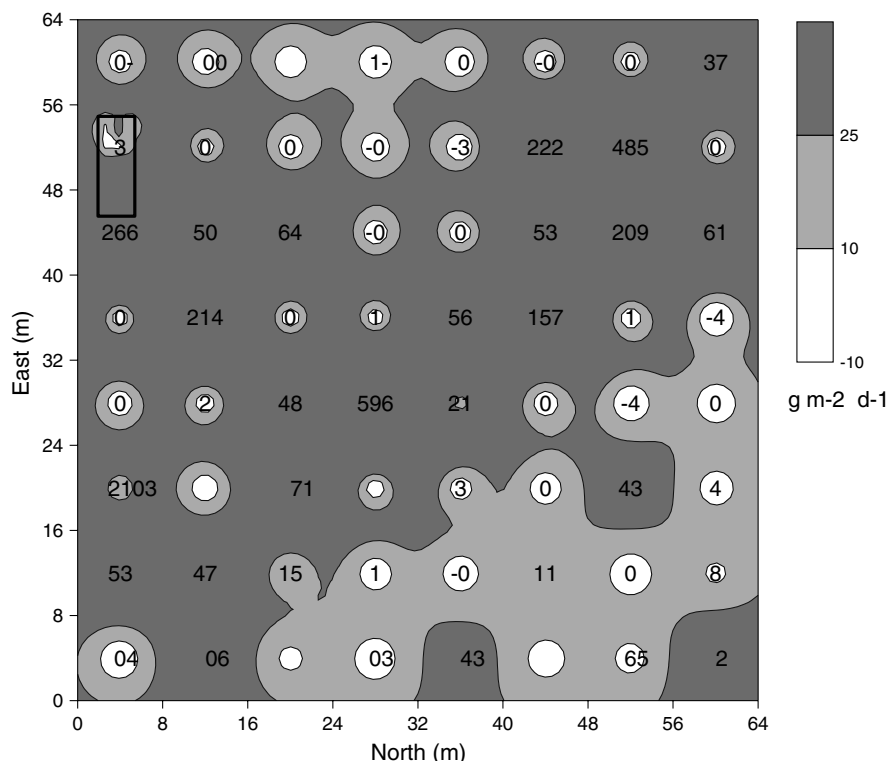


Fig. 3. S4-Grid Flux ($\text{g m}^{-2} \text{d}^{-1}$) contours obtained using inverse distance weighing. * The rectangle indicates the close-sampling area with 12 flux locations.

360 The geospatial mean flux was $21.6 \text{ g m}^{-2} \text{d}^{-1}$ for the
 361 S1-Grid and $50.0 \text{ g m}^{-2} \text{d}^{-1}$ for the S4-Grid, similar to
 362 the means obtained (Table 1). Three relative zones were
 363 classified based upon methane emission contours at these
 364 sites, low ($<10 \text{ g m}^{-2} \text{d}^{-1}$), medium ($10\text{--}25 \text{ g m}^{-2} \text{d}^{-1}$),
 365 and high ($>25 \text{ g m}^{-2} \text{d}^{-1}$). The S1-Grid had a larger zone
 366 with relatively low emissions (30.6%) as compared to the
 367 S4-Grid (4.8%). High emission zones represented 67.4%
 368 of the S4-Grid and 23.6% of the S1-Grid (Table 3). High
 369 emission zones in the S1-Grid were isolated spots
 370 (Fig. 2). In contrast, high emission zones in the S4-Grid
 371 were continuous and represented 67.4% of the total emis-
 372 sions area (Fig. 3). The contours also show that emissions
 373 from one-third of the thicker intermediate cover were clas-
 374 sified as low emission zones as compared to only 4.8% of
 375 the daily cover area.

Table 3
 Summary of geospatial results

	S1-Grid	S4-Grid
Total area (m^2)	3697	4096
Geospatial mean ($\text{g m}^{-2} \text{d}^{-1}$) ^a	21.61	50.0
Total methane emissions (kg/day)	80	205
Low flux area (% area)	30.6	4.8
Medium flux area (% area)	45.8	27.8
High flux area (% area)	23.6	67.4

^a Volume under model surface divided by surface area obtained using IDW.

376 Contrasting the results shown in Tables 1 and 3, one can
 377 see that the differences in the numbers of high, medium, and
 378 low fluxes measured on the S1-Grid and the S4-Grid are not
 379 as significant as the differences in areas of high, medium,
 380 and low emissions shown in Table 3. This observation indi-
 381 cates that even though both sites have similar numbers of
 382 varying fluxes, the patterns of emissions from the S1-Grid
 383 and the S4-Grid are quite different. The pattern of emission
 384 is a function of how these emissions vary with space.

385 These differences in flux patterns suggest that different
 386 treatments should be used to mitigate methane emissions
 387 at different types of sites as represented by these two covers.
 388 Alternatively, differing treatments could be based on mea-
 389 sured patterns of emissions. For example, landfill CH_4 emis-
 390 sions from covers similar to the S1-Grid (relatively thick and
 391 well-vegetated, and having isolated CH_4 hot spots) can most
 392 easily be reduced by placing individualized biocovers only on
 393 high emission areas typically referred to as “hot spots.” Bio-
 394 covers are layers of compost overlaying a porous dispersing
 395 layer (Huber-Humer, 2004). Such “hot spots” may be iden-
 396 tified using a portable FID (Flame Ionization Detector). On
 397 the other hand, emissions from sites with thin intermediate
 398 covers are best mitigated by applying a layer of compost
 399 overlaying a porous dispersing layer (biocover) across the
 400 whole surface. A biocover applied over a thin intermediate
 401 cover can then be either stripped and then re-applied over
 402 the new active phase or left as part of the existing cover, as
 403 when there is an abundance of yard waste (Florida).

404 4. Summary and conclusions

405 Methane flux emissions were measured on two surfaces
 406 at a solid waste landfill. One surface was a thick intermedi-
 407 ate well-vegetated soil cover and the other a thin interme-
 408 diate non-vegetated soil cover. Both types of covers are
 409 significant sources of greenhouse emissions. Emissions
 410 from the thin cover were double the emissions from the
 411 thicker well-vegetated soil cover. Methane oxidation
 412 through the cover was only partly responsible for the lower
 413 emissions from the thicker cover. Mapping of the surface
 414 fluxes shows that the patterns of emission from each cover
 415 were different. Mitigation of emissions from the thin inter-
 416 mediate cover can best be achieved by placing a compost-
 417 amended biocover on the entire area. On the other hand,
 418 for a thicker well-vegetated intermediate cover, compost
 419 placement can be limited to high emission zones.

420 5. Uncited reference

421 [Bogner et al. \(1995\).](#)

422 Acknowledgments

423 Financial support for the study described in this paper
 424 was provided by the Florida Center of Solid and Hazard-
 425 ous Waste Management (FCSHWM), the National Science
 426 Foundation (NSF), under Grant No. 0093677, and Waste
 427 Management Inc. Testing was performed at the Leon
 428 County Landfill, Tallahassee, Florida (USA). Invaluable
 429 assistance was provided by Jud Curtis, Norm Thomas,
 430 Nancy Paul, and DJ Newsom, Leon County Solid Waste
 431 Officials. Their efforts on behalf of the project are greatly
 432 appreciated. The findings described in this paper are solely
 433 those of the authors. Endorsement by FCSHWM, NSF, or
 434 Leon County, Florida is not implied.

435 References

436 Abichou, T., Powelson, D., Chanton, J., Escoriza, S. 2005. Character-
 437 ization of methane oxidation at a solid waste landfill. *Journal of*
 438 *Environmental Engineering*, ASCE (accepted).
 439 Barker, J., Fritz, P., 1981. Carbon isotope fractionation during microbial
 440 methane oxidation. *Nature* 293, 289–291.
 441 Barlaz, M., Green, R., Chanton, J., Goldsmith, C., Hater, G., 2004.
 442 Evaluation of a biologically active cover for mitigation of landfill
 443 gas emissions. *Environmental Science and Technology* 38, 4891–
 444 4899.
 445 Bergamaschi, P., Lubina, C., Konigstedt, R., Fischer, H., Veltkamp, A.,
 446 Zwaagstra, O., 1998. Stable isotopic signatures ($d^{13}C$, dD) of methane
 447 from European landfill sites. *Journal of Geophysical Research* 103
 448 (D7), 8251–8266.
 449 Bogner, J., Matthews, E., 2003. Global methane emission from landfills:
 450 new methodology and annual estimates 1980–1996. *Global Biogeo-*
 451 *chemical Cycles* 17 (2), 1065–1083.
 452 Bogner, J., Spokas, K., 1993. Landfill CH_4 : rates, fates and role in global
 453 carbon cycle. *Chemosphere* 26, 369–386.
 454 Bogner, J., Spokas, K., Burton, E., Sweeney, R., Corona, V., 1995.
 455 Landfills as atmospheric methane sources and sinks. *Chemosphere* 31,
 456 4119–4130.

Bogner, J., Meadows, M., Czepiel, P., 1997. Fluxes of CH_4 between
 457 landfills and the atmosphere: natural engineered control. *Soil Use and*
 458 *Management* 3, 268–277.
 459 Borjesson, G., Svensson, B., 1997. Seasonal and diurnal methane
 460 emissions from a landfill and their regulation by methane oxidation.
 461 *Waste Management and Research* 15, 33–54.
 462 Borjesson, G., Chanton, J., Svensson, B., 2001. Methane oxidation in two
 463 Swedish landfill cover soils determined with the use of $^{13}C/^{12}C$ isotope
 464 ratios. *Journal of Environmental Quality* 30, 369–376.
 465 Chanton, J., Liptay, K., 2000. Seasonal variation in methane oxidation in
 466 a landfill cover soil as determined by an in situ stable isotope
 467 technique. *Global Biogeochemical Cycles* 14, 51–60.
 468 Chanton, J.P., Rutkowski, C.M., Mosher, B.M., 1999. Quantifying
 469 methane oxidation from landfills using stable isotope analysis of
 470 downwind plumes. *Environmental Science and Technology* 33, 3755–
 471 3760.
 472 Christophersen, M., Holst, H., Kjeldsen, P., Chanton, J., 2001. Lateral gas
 473 transport in a soil adjacent to an old landfill: factors governing
 474 emission and methane oxidation. *Waste Management and Research*
 475 19, 126–143.
 476 Coleman, D., Risatti, J., Schoell, M., 1981. Fractionation of carbon and
 477 hydrogen isotopes by methane-oxidizing bacteria. *Geochimica et*
 478 *Cosmochimica Acta* 45, 1033–1037.
 479 Czepiel, P., Mosher, B., Crill, P., Harriss, R., 1996. Quantifying the effects
 480 of oxidation on landfill methane emissions. *Journal of Geophysical*
 481 *Research* 101, 16721–16729.
 482 Czepiel, P., Shorter, J., Mosher, B., Allwine, E., McManus, J., Harriss, R.,
 483 Kolb, C., Lanb, B., 2003. The influence of atmospheric pressure on
 484 landfill methane emissions. *Waste Management* 23 (7), 593–598.
 485 De Visscher, A., De Pourcq, J., Chanton, J., 2004. Isotope fractionation
 486 effects by diffusion and methane oxidation in landfill cover soils.
 487 *Journal of Geophysical Research* 109 (D18). Art. No. D18111.
 488 Dlugokencky, E., Masarie, K., Lang, P., Tans, P., Steele, L., Nisbet, E.,
 489 1994. A dramatic decrease in the growth rate of atmospheric methane
 490 in the northern hemisphere during 1993. *Geophysical Research Letters*
 491 21, 45–48.
 492 Dlugokencky, E., Masarie, K., Lang, P., Tans, P., 1998. Continuing
 493 decline in the growth rate of atmospheric methane burden. *Nature* 393,
 494 447–450.
 495 Etheridge, D., Steele, L., Francey, R., Langenfelds, R. 1998. Atmospheric
 496 methane between 1000 AD and present: Evidence of anthropogenic
 497 emissions and climatic variability.
 498 Fung, I., Lerner, J., Matthews, E., Prather, M., Steele, L., Fraser, P., 1997.
 499 Three-dimensional model synthesis of the global methane cycle.
 500 *Journal of Geophysical Research* 96, 13033–13065.
 501 Hogan, K. 1993. Anthropogenic methane emissions in the US. Estimates
 502 For 1990, Report to Congress. US Environmental Protection Agency.
 503 Washington, DC, April 1993.
 504 Huber-Humer, M. 2004. Abatement of landfill methane emissions by
 505 microbial oxidation in biocovers made of compost. Ph.D. Dissertation.
 506 Universität für Bodenkultur Wien, Austria.
 507 IPCC, 2001. *Climate Change 2001: The Scientific Basis*. Contribution of
 508 working group I to the 3rd assessment report of the intergovernmental
 509 panel on climate change. Cambridge University Press, United King-
 510 dom and New York.
 511 Lelieveld, J., Crutzen, P., Dentener, F., 1998. Changing concentration,
 512 lifetime, and climate forcing of atmospheric methane. *Tellus B* 50, 128–
 513 150.
 514 Liptay, K., Chanton, J., Czepiel, P., Mosher, B., 1998. Use of stable
 515 isotopes to determine methane oxidation in landfill cover soils. *Journal*
 516 *of Geophysical Research* 103, 8243–8250.
 517 Livingston, G.P., Hutchinson, G., 1995. Enclosure-based measurement of
 518 trace gas exchange: applications and sources of error. In: Matson,
 519 P.A., Harriss, R.C. (Eds.), *Methods in Ecology, Biogenic Trace Gases:*
 520 *Measuring Emissions from Soil and Water*. Blackwell Science,
 521 Cambridge, MA., pp. 14–52.
 522 Merritt, D., Hayes, J., Des Marais, D., 1995. Carbon isotopic analysis of
 523 atmospheric methane by isotope-ratio-monitoring gas-chromatography
 524

- 525 mass-spectrometry. *Journal of Geophysical Research* 100 (D1), 1317–
526 1326.
- 527 Spokas, K., Graff, C., Morcet, M., Aran, C., 2003. Implications of the
528 spatial variability on landfill emission rates on geospatial analyses.
529 *Waste Management* 23, 599–607.
- 530 Surfer, 2002. *Surfer 8 User's Guide*. Golden Software, Inc., Golden, CO.
- Thompson, A., Hogan, K., Hoffman, J., 1992. Methane reductions:
implications for global warming and atmospheric chemical change.
Atmospheric Environment A 26, 2665–2668.
- Yates, S., Warrick, A., 2002. Geostatistics. In: Dane, J.H., Topp, G.C.
(Eds.), *Methods of Soil Analysis. Part 4-Physical methods*. Soil Science
Society of America, Madison, WI, pp. 81–118.

531
532
533
534
535
536
537

UNCORRECTED PROOF